Available online at www.sciencedirect.com
ScienceDirect
International Journal of Refrigeration 30 (2007) 946–957
REVUE INTERNATIONALE DU FROID
INTERNATIONAL JOURNAL OF
refrigeration
www.elsevier.com/locate/ijrefrig

Wall and fluid inlet temperature effect on heat transfer in incompressible laminar oscillating flows

Philippe Nika*, Yannick Bailly[1], François Guermeur[2], François Lanzetta[3]

Département CREST FEMTO-ST/UMR CNRS 6174, Parc technologique, 2, avenue Jean Moulin, 90000 Belfort, France

Received 23 January 2006; received in revised form 31 October 2006; accepted 30 January 2007
Available online 12 February 2007

Abstract

This paper deals with the problem of oscillating flows occurring in devices such as Stirling or thermoacoustic engines and refrigerators. Since the global governing equations cannot be solved, the authors propose to introduce a few simplifications; the most simplifying reduction is that the fluid is assumed to be incompressible. However, specific attention is paid to describing the flow characteristics that's why the Lagrangian formalism which allows the individual study of each fluid particle is adopted. Thereby each particle contribution to global thermal effects can be evaluated and the gas temperature profiles along the exchanger can be computed. Various situations are presented including the case of a non-uniform temperature at the wall and a phase lag between pressure and temperature at the fluid entrance. The efficiency of the wall to fluid thermal exchange is analyzed. The authors show that this exchange depends upon two important parameters: the geometric ratio between the exchanger length and the particle oscillating displacement, and a thermal parameter "β", governing the temperature profiles and related to the Prandtl number, the operating frequency and the phase lag between the instantaneous heat flux and the wall to fluid temperature difference.
© 2007 Elsevier Ltd and IIR. All rights reserved.

Keywords: Thermoacoustic; Pulse tube; Stirling; Research; Heat transfer; Laminar flow; Periodic phenomenon; Wave; Parameter; Temperature; Efficacy; Heat exchange

Effet des températures d'entrée de fluide et des températures de paroi sur l'échange thermique d'un fluide incompressible en écoulement oscillant

Mots clés : Thermoacoustique ; Tube à pulsation ; Stirling ; Recherche ; Transfert de chaleur ; Écoulement laminaire ; Phénomène périodique ; Onde ; Paramètre ; Température ; Efficacité ; Échange de chaleur

* Corresponding author. Tel.: +33 03 84 57 82 04; fax: +33 03 84 57 00 32.
E-mail addresses: philippe.nika@univ-fcomte.fr (P. Nika), yannick.bailly@univ-fcomte.fr (Y. Bailly), francois.guermeur@univ-fcomte.fr (F. Guermeur), francois.lanzetta@univ-fcomte.fr (F. Lanzetta).
[1] Tel.: +33 03 84 57 82 08.
[2] Tel.: +33 03 84 57 82 08.
[3] Tel.: +33 03 84 57 82 24.

0140-7007/$35.00 © 2007 Elsevier Ltd and IIR. All rights reserved.
doi:10.1016/j.ijrefrig.2007.01.011

Nomenclature

c	specific heat capacity at constant pressure ($J\,kg^{-1}\,K^{-1}$)
C_f	friction factor
D	gas displacement (m)
d_h	hydraulic diameter (m)
e	thickness (m)
E	exchange effectiveness
F_1, F'_1	functions Eqs. (22) and (34)
H	convection heat coefficient ($W\,m^{-2}\,K^{-1}$)
$\dot{h}, \dot{H}$	local and radial average of enthalpy flux ($W\,m^{-2}$)
j	complex imaginary ($j^2 = -1$)
l	length (m)
Nu, Nu_{R1}, Nu_{I1}	Nusselt number, real part, imaginary part
P	pressure (Pa)
Pr	Prandtl number
Q	thermal energy (J)
Re	Reynolds usual number
S_{pass}	internal cross-section (m^2)
T	time (s)
T	temperature (K)
$t^* = \omega t$	non-dimensional time
u, v	velocities for x and y directions ($m\,s^{-1}$)
$u^* = (2u/\omega D)$	non-dimensional fluid velocity
W_{om}	Womersley/Stokes number
x	axial coordinate (m)
$x^* = (x/(l_0/2))$	non-dimensional axial coordinate
y, z	co-ordinates (m)
$y^* = (y/(e/2))$	non-dimensional co-ordinates

Greek

λ	parameter Eq. (11)
λ_i	thermal conductivity i ($W\,m^{-1}\,K^{-1}$)
μ	dynamic viscosity ($kg\,m^{-1}\,s^{-1}$)
ρ	density ($kg\,m^{-3}$)
ω	pulsation ($rad\,s^{-1}$)
ξ	Lagrangian variable
Δ	thermal gradient ($K\,m^{-1}$)
ΔT_{rad}	radial gradient $T_g - T_{-1}$ (K)
ΔT_{long}	longitudinal gradient $T_1 - T_{-1}$ (K)
Λ_L	fluid relative displacement

Subscripts and superscripts

g	gas
in, in′	entrance in $x^* = -1$ and in $x^* = 1$
l_0	extremity in $x = l_0$
rad, long	radial and longitudinal
t	tube
0	initial, for $x = 0$, of reference
out, out′	Exiting in $x^* = -1$ and in $x^* = 1$
1, −1	to right or left extremity

Operators

p^*, T^*	normalized magnitude with respect to reference value p_0, T_0
$\Im$	imaginary part
$\Re$	real part
$\overline{x}$	x cross-section average
$\|x\|$	x magnitude
$\langle x \rangle$	x temporal average on a semi-period

1. Introduction

Numerous varieties of thermal machines operate with an internal oscillating fluid flow: Stirling cooler [1], all type of Stirling engines including the kinematic engines and the free piston or free displacer engines: Martini model [2], Ringbom model [3] and hot air flow engine like Manson model. All versions of Pulse Tube Refrigerators (PTR, OPTR, DIOPTR [4,5], etc.) and thermoacoustic systems based on standing or progressive waves (Ceperley ring [6]) are also concerned. There are also a lot of hybrid systems like Gifford-Mc Mahon and Vuilleumier coolers [7] or fluidynes pumps and liquid piston Stirling machines [8,9]. All these machines are known for many years but are not of a common use yet. However, they may take a bigger place in a near future because of their abilities to operate with various energy sources brought by external ways (hence removing most technical problems occurring in internal combustions): biogas, solar energy, geothermic, heat collected downstream industrial processes, and thermoacoustic waste heat upgrading.

In most cases, the mechanical conception of these machines is quite simple compared to gas turbines, internal combustion engines or classic refrigerating and gas liquefaction devices. Note that some of them (purely thermoacoustic devices) do not require any mobile part. In this paper the authors propose to focus their interest on a particular part of these systems: the heat exchangers where at least one fluid operates in oscillating flow mode. Moreover, such devices can improve many industrial processes; for example numerous works [10,11] show the interest of oscillating flows in micro-heat exchangers used as coolers for electronic components.

The oscillating fluid flow causes thermal exchange phenomena which are not well estimated yet. Indeed, due to a lack of knowledge, most researchers and engineers use classic heat exchangers calculus, assuming fluids moving in a steady state flow regime which is not in connection with reality. As mentioned above, very few theoretical or

experimental studies concerning oscillating flows in heat exchangers have been developed during the past decades. That's the reason why Gedeon [12] and Swift [13] can be considered as precursors. More recently Wakeland and Keolian [14–16] propose some interesting results on thermal transfers between two exchangers in a standing wave acoustic field. Similarly, in a precedent paper [17,18], the authors point out two fundamental aspects for designing such devices: first the exchangers length in oscillating flow mode must be equal to the fluid peak to peak displacement and second, the temperature gradient at the wall may introduce a "regenerator effect". In the latter consideration, a fluid particle may exchange with the wall a heat quantity exactly equal to the heat quantity it will reload at the same location when flowing in the opposite direction, hence the global thermal effect is null. In fact, the main parameters of interest for describing laminar and quasi incompressible flows are the fluid relative motion Λ_L, which depends of the mechanic configuration and the Womersley number W_{om}, which is linked to the operating frequency [17]. The Womersley number represents in fact the ratio of inertial forces to viscous forces in non-stationary regime, it is also an information on the relative thickness of dynamical viscous boundary layers compared to hydraulic radius of the canal.

$$W_{om} = \sqrt{\frac{\rho_0 \omega r_h^2}{\mu}} \tag{1}$$

In addition complex forms of Nusselt numbers are used to characterize the heat transfers between walls and oscillating fluids. This allows the introduction of the phase lag between temperature variation and wall thermal exchange.

The present paper is an extension of Ref. [17]: after a brief description of the most significant modeling steps and general results, the authors emphasize the discussion on the effects of temperature gradient at the wall and fluid temperature which may vary over time at the entrance as it is the case in systems cited previously. In order to obtain a more realistic behavior of engine with oscillating flow, as mentioned previously, the influence of temporal variations of the inlet fluid temperature and its phase lag with pressure is particularly discussed in this study.

2. Overview and model parameters

2.1. One-dimensional problem

The considered heat exchangers are currently made of many parallel channels so the basic geometry consists of two plane-parallel plates with an inter-plate space e. The channel height (see Fig. 1) is considered as infinite in the z direction and the length is limited to l_0 in the x direction.

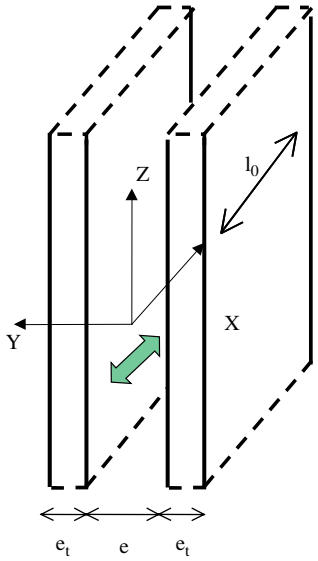

Fig. 1. Basic studied geometry, oscillating flow in the x direction.

Solid walls may have a temperature gradient along x which generates thermal coupling phenomena between the oscillating fluid and the walls.

The oscillatory motion considered takes place along the x direction and has an amplitude "D". In Ref. [17] the authors show that general two-dimensional equations for the flow and temperatures can be reduced to a one-dimensional physical model in the x direction as the system is supposed infinite in the z direction. The method consists in averaging fluid velocity and temperature in the y direction, $(\overline{u}, \overline{T}_g) = (1/2e)\int_{-e/2}^{e/2} (u, T_g)\mathrm{d}y$ so the model [17] describes the averaged values of physical parameters (p, T, ρ, u, etc.) within any (y, z) section. Thereby, it is necessary to introduce friction factor and heat transfer coefficients for the wall boundary values. In the model, the thermo-physical properties of fluid and material are also assumed to be temperature independent. All parameters introduced during the non-dimensional treatment are listed in Appendix 1. Spatio-temporal evolutions of fluid temperature depend both on fluid/wall thermal transfer coefficients and thermal conditions at plates' extremities: end of solid wall, mixing of fluid, connected devices, and existing heat exchangers. All these parameters are functions of the relative particle displacement Λ_L and of the plate length l_0. As explained, we have to introduce in the 1D model different correlations for channel geometry and to take into account pressure losses as well as oscillatory heat transfer boundary conditions at the wall.

The wall friction factor C_f and the fluid to plate thermal transfer coefficient h are both expressed by means of a complex form in order to introduce two phases: the phase lag between fluid velocity and wall stress and the phase lag

between thermal flux and fluid/wall temperature difference that may occur in oscillating flow mode [19]:

$$C_f = -\frac{2\mu}{\overline{\rho}}\frac{\left.\frac{\partial u}{\partial y}\right|_{e/2}}{|\overline{u}|\overline{u}} \tag{2}$$

and

$$Nu = \frac{hd_h}{\lambda_g} = -d_h\frac{\left.\frac{\partial T}{\partial y}\right|_{e/2}}{\left(T_t|_{e/2} - \overline{T}_g\right)} \tag{3}$$

These formulations are detailed in the previous paper [17]; parietal and mean values of velocity or temperature are complex, as usual in linear thermoacoustics. The forms $u = u_0\widehat{f}_y e^{j\omega t}$ and $\overline{u} = u_0\widehat{g}e^{j\omega t}$ are adopted, where the two functions $\widehat{f}_y, \widehat{g}$ are depending on the canal geometry. Real and imaginary parts of C_f and Nu were calculated in [18] for rectangular channels and represented versus the Womersley number.

In the correlations for C_f and Nu, the Reynolds number can conventionally be based on the hydraulic diameter d_h ($d_h = 2e$ for two infinite planes) and on the axial velocity magnitude:

$$Re = \frac{d_h\overline{\rho}_g|\overline{u}|}{\mu_g} \tag{4}$$

Hence, in the non-dimensional form (stared notation), boundary conditions at the walls for velocities and thermal flux can be expressed by these more appropriate forms:

$$\left.\frac{\partial u^*}{\partial y^*}\right|_{y^*=1} = -\frac{Re}{8}\left(\Re[C_f]\overline{u}^* + \Im[C_f]\frac{\partial\overline{u^*}}{\partial t^*}\right) \tag{5}$$

$$\lambda_g\left.\frac{\partial T_g^*}{\partial y^*}\right|_{y^*=1} = \lambda_t\left.\frac{\partial T_t^*}{\partial y^*}\right|_{y^*=1} = \Re[h]\left(\overline{T}_t^* - \overline{T}_g^*\right) + \frac{\Im[h]}{\omega}\frac{d\left(\overline{T}_t^* - \overline{T}_g^*\right)}{dt^*} \tag{6}$$

With the assumption of an incompressible fluid ($\rho^* = 1$) in an oscillating flow mode between two plates, the characteristic equations of the problem are detailed in Ref. [17]:

Fluid velocity is uniform along the canal and time dependent:

$$\overline{u}^* = \frac{2u}{\omega D} = \cos t^* \tag{7}$$

Equation for the pressure drop (not analyzed in this work):

$$\frac{4\Lambda_L}{M_\omega^2}\frac{\partial p^*}{\partial x^*} = \left(1 + \frac{\Im[C_f]Re}{8W_{om}^2}\right)\sin t^* - \frac{\Re[C_f]Re}{8W_{om}^2}\cos t^* \tag{8}$$

Equation of the fluid energy (basis of the present study):

$$\left(\left(1 + \frac{Nu_{I1}}{4PrW_{om}^2}\right)\frac{\partial\overline{T}_g^*}{\partial t^*} + \Lambda_L\cos t^*\frac{\partial\overline{T}_g^*}{\partial x^*} + \frac{Nu_{I1}}{4PrW_{om}^2}\overline{T}_g^*\right) = \frac{1}{4PrW_{om}^2}\left[Nu_{R1}\overline{T}_t^* + Nu_{I1}\frac{d\left(\overline{T}_t^*\right)}{dt^*}\right] \tag{9}$$

A usual simplification (see Section 2.3) consists in imposing a constant linear temperature at the wall:

$$T_t^* = \frac{T_1^* - T_{-1}^*}{2}x^* + \frac{T_1^* - T_{-1}^*}{2} \tag{10}$$

where T_1 and T_{-1} are imposed wall temperature at extremities (see Fig. 2)

Boundary conditions for the flow are taken as:

$$x^* = -1,\ \overline{U}^* = \cos t^*,\ T_g^*(t,-1) = T_{g-1} \tag{11}$$

$$x^* = -1,\ \overline{U}^* = \cos t^*,\ T_g^*(t,1) = T_{g+1} \tag{12}$$

Eqs. (11) and (12) postulate that when fluid enters the canal at $x^* = -1$ (left side in Fig. 2) or at $x^* = 1$ (right side in Fig. 2) it is at a uniform temperature but this temperature may depend over time (Section 2.4)

To solve the energy equation, the x Eulerian variable is replaced by the Lagrangian variable:

$$\xi = x^* - \lambda\sin t^* \tag{13}$$

Then, the following two parameters are introduced (see other numbers' definitions in Appendix 1):

$$\lambda = \frac{4PrW_{om}^2\Lambda_L}{Nu_{I1} + 4PrW_{om}^2} \tag{14}$$

$$\beta = \frac{Nu_{R1}}{Nu_{I1} + 4PrW_{om}^2} \tag{15}$$

Finally, Eq. (9) can be summarized by the following general form:

$$\frac{\partial\overline{T}_g^*}{\partial t^*} + \beta\overline{T}_g^* = \beta\overline{T}_t^*(\xi + \lambda\sin t^*) \tag{16}$$

The β parameter depends on the imaginary part of the heat transfer Nu_{I1}, on the Prandtl and Womersley numbers and characterizes (Eq. (22)) the phase lag of the fluid to wall heat transfer. The λ parameter is important when wall temperature is not uniform, so it characterizes the "regenerator" effect in that case, i.e. possibility for the wall to restitute to the fluid the heat deposited along the previous semi-period.

The evolutions of the two parameters (λ/Λ_L) and β as a functions of W_{om} have been studied on Fig. 3 in Ref. [17]. The Prandtl number has the value $Pr = 0.7$ and the Nusselt numbers Nu_{R1} and Nu_{I1} are estimated by using

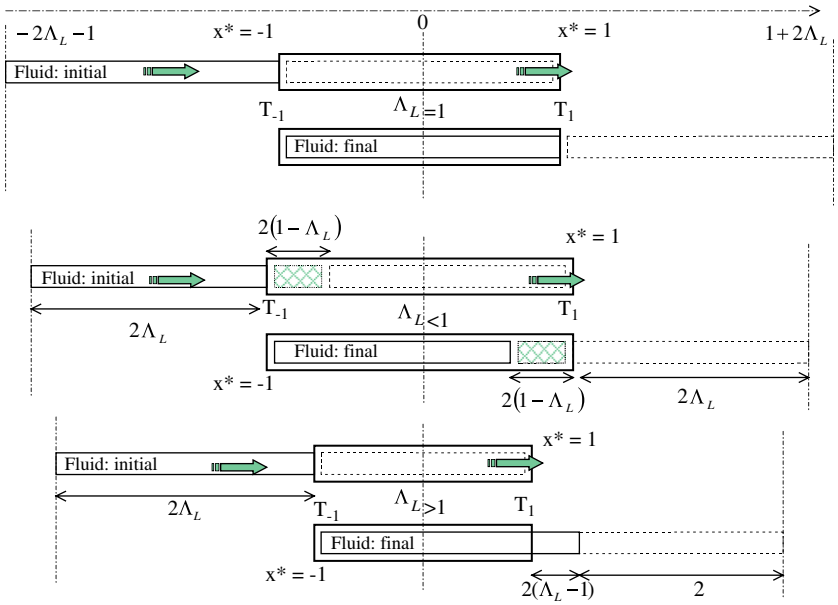

Fig. 2. Description of the oscillating flow in the x direction according to the ratio Λ_L. The scheme represents half an alternation of the fluid displacement. The central rectangular box is the volume between two plates of the heat exchanger. The fluid flows from the left (initial position) to the right (final position). From top to bottom, $\Lambda_L = 1$ stands for heat exchanger where displacement of fluid is equal to exchanger length, $\Lambda_L < 1$ for long exchangers and $\Lambda_L > 1$ for short exchangers.

relations given in Appendix 1 [17]. For W_{om} varying from 0 to 50 (λ/Λ_L) varies between 0.835 and 1 because the imaginary part of Nusselt number has a week influence. β quickly decreases when W_{om} increases: since $W_{om} > 1.3$ and $\beta < 2$, W_{om} and β decrease asymptotically to 0.

2.2. Case of a constant and uniform wall temperature $\overline{T}_t^* = 1$

In most real cases, "entrance" fluid temperatures (and also the pressures), on the two extremities T_{g-1}, T_{g1} for non-dimensional co-ordinates $x^* = -1$ and $x^* = 1$, vary over time and are out of phase with respect to fluid displacement. In a first step, in order to facilitate understanding, we consider their values as constant and not time dependent; variations over time will be discussed lately. The arbitrary choice of a hot fluid temperature at the left inlet $(x^* = -1)$ and a cold one at the right inlet $(x^* = 1)$ is made; the wall temperature is kept constant and uniform.

For constant boundary conditions, the solution for gas temperature is quite simple:

$$\Delta T_{rad}(t^*, \xi) = \left(\overline{T}_g^*\left(t_{in}^*, \xi\right) - 1\right) e^{-\beta(t^* - t_{in}^*)} \tag{17}$$

where t_{in}^* corresponds to the fluid particle entrance time at $x^* = -1$ and $\Delta T_{rad}(t^*, \xi) = \overline{T}_g^*(t^*, \xi) - \overline{T}_t^*$ is the fluid to wall temperature difference in Lagrangian formalism ξ at time t^* and along the system.

Thereby, Eq. (17) represents the history of the temperature difference between the gas and the wall. If the considered gas particle comes from the initial position x_0^*, at time t_0^*, and enters into the plates at time t_{in}^*, its position at any time t^* is then given by:

$$x^* = x_0^* + \Lambda_L(1 + \sin t^*) \tag{18}$$

Eq. (17) is only valid between t_{in}^* and t_{out}^*, the latter instants defining the times when the fluid particle remains within the system. t_{in}^* and t_{out}^* are given by:

$$t_{in}^* = \arcsin\left(-1 - \frac{\left(1 + x_0^*\right)}{\Lambda_L}\right) \tag{19}$$

$$t_{out}^* = 2t_0^* + 2\pi - t_{in}^* \tag{20}$$

The temperature difference provided by Eq. (17) appears indirectly as a function of the fluid displacement along the plates by the value of the fluid where the non-dimensional particle position x^* is masked by the Lagrangian variable ξ (see Eq. (13)). Moreover, due to thermal transfers between plates, an exponential decrease (β parameter) of the initial (in $x^* = -1$) wall to fluid thermal difference ΔT_{rad} is observed, suggesting an optimal exchanger length may exist for a maximal heat transfer.

In fact, the fluid particles located between the plates and initially located at $x_0^* > -1$ (if time origin is $t_0^* = -(\pi/2)$, and then $u^* = 0$) never reach the position $x^* = -1$ because their displacement is on the right. On the other hand,

according to the particle displacement value Λ_L, a part of these particles moves up to $x^* = +1$ (see Fig. 2).

To simplify and to clarify the discussion, we first consider the fluid particle that enters a well mixed and constant temperature tank on both sides of the canal. At $t^* = t_0^* + \pi$, the direction of the fluid particle changes so the movement occurs from $x^* = 1$ to $x^* = -1$. In the model presented here, the fluid particles flowing back (cold fluid) into the exchanger at $x^* = 1$ are considered to be at a temperature inferior of $\Delta T_{\mathrm{rad}(+1)} = -0.75$ to that of wall, and those (hot fluid) flowing into the exchanger at $x^* = -1$ to be at a temperature $\Delta T_{\mathrm{rad}(-1)} = +0.75$. In the case of the relative displacement of fluid particle which is less than unity ($\Lambda_L < 1$), a part of fluid remains inside the exchanger forever and never flows out. Therefore, its temperature reaches the wall temperature exponentially over time (Eq. (17)). This fluid part forms a "fluid stopper" zone that does not contribute to any global thermal exchange.

Fig. 3 shows the modification of the fluid temperature profile along the plates for three exchanger geometries: short $\Lambda_L = 1.5$, with a length equal to fluid displacement $\Lambda_L = 1$ and long $\Lambda_L = 0.5$. The results are presented considering the thermal parameter $\beta = 0.5$. Hot fluid enters the exchanger at constant temperature at $x^* = -1$ and cold fluid in the reversed flow at $x^* = 1$. Straight lines represent, time after time, the fluid temperature profiles during the movement from left to right, and dotted lines, the profiles corresponding to the movement in the opposite direction. One can clearly observe the exponential decrease of the thermal discontinuity front occurring time after time during the fluid progression. In Fig. 5 of [17], it is shown that the smaller β is (for large W_{om} values), the bigger the observed temperature front (since fluid entrance) is, i.e. gas/wall temperature difference remains high hence indicating that thermal transfers are quite bad probably. This clearly indicates that the rate of the thermal front decreases, thus exchanger efficiency depends upon Λ_L. In fact, only fluid particles reaching both the exchanger extremities at $x^* = -1$ and $x^* = 1$ are able to exchange heat with the wall.

Here on Fig. 3, for a similar absolute fluid displacement, one notes that a too long exchanger ($\Lambda_L = 0.5$) has an inactive zone for both hot and cold fluid, respectively, between $x^* = -1$ and 0 and $x^* = 0$ and $+1$. On the contrary a too short exchanger ($\Lambda_L = 1.5$) does not permit a maximum heat extraction. In fact, "exit" temperatures at $x^* = +1$ and "return" temperatures at $x^* = -1$ are higher in such an exchanger.

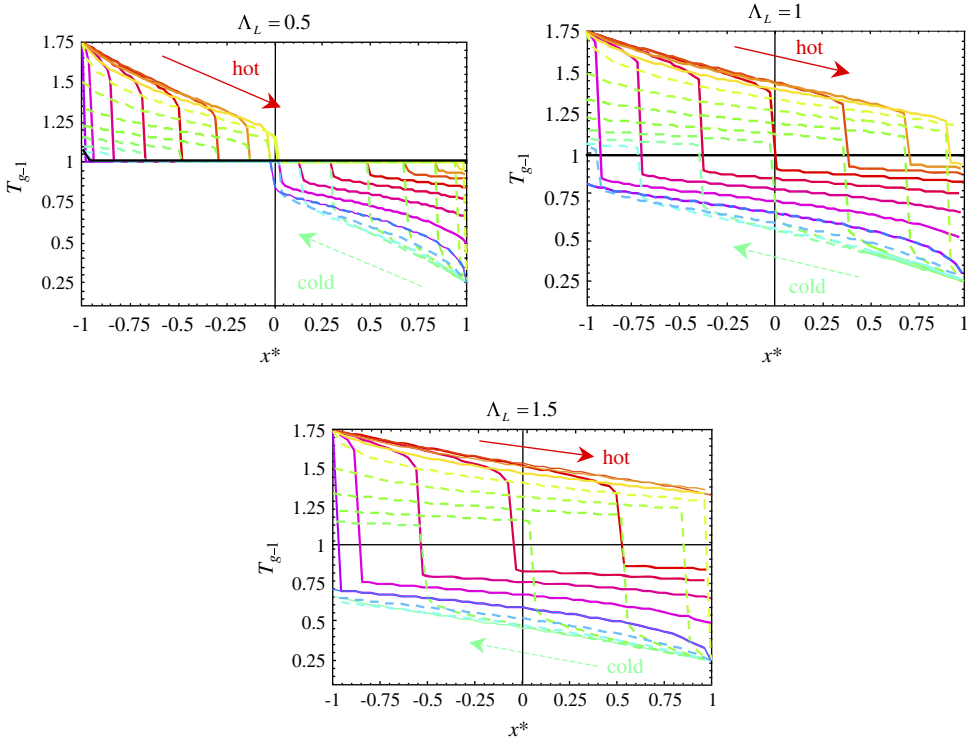

Fig. 3. Histories of the non-dimensional temperature profile along the exchanger $[-1, +1]$ and of the relative fluid displacement, case of a constant wall temperature $\Delta T_{\mathrm{long}} = 0$ (horizontal thick line). Hot fluid inlet $\Delta T_{\mathrm{rad}(-1)} = 0.75$ on the left on the first half alternation, and cold fluid inlet on the right $\Delta T_{\mathrm{rad}(1)} = -0.75$ on the reciprocating flow. Full lines represent a flow period from $x^* = -1$ to $x^* = +1$, dotted lines in the other way – $\beta = 0.5$ and $Pr = 0.7$. $\Lambda_L = 1$ stands for heat exchanger where displacement of fluid is equal to exchanger length, $\Lambda_L < 1$ for long exchangers and $\Lambda_L > 1$ for short exchangers.

After some tedious calculus [17], the global heat quantity exchanged between fluid and plates during half period (left to right for example) can be expressed by:

$$Q_{\text{rad}} = \rho c_g S_{\text{pass}} T_0 \Delta T_{\text{rad}(-1)} \frac{l_0}{2} \Lambda_L F_1(\beta) \tag{21}$$

where F_1 is defined by:

$$F_1(\beta) = \frac{1 + 8\beta^2 - e^{-2\beta\pi}}{1 + 4\beta^2} \tag{22}$$

Since the maximum heat quantity that could be exchanged by the gas along its displacement through the exchanger is $Q_{\max\, i} = \rho c_g D S_{\text{pass}} T_0 \Delta T_{\text{rad}(-1)}$, the function $(1/2)F_1$ represents the exchanger effectiveness value: $E = (Q_{\text{rad}}/Q_{\max\, i}) = (1/2)F_1$. Fig. 4 shows this effectiveness as a function of β parameter: the maximal value of 100% is reached for $\beta > 2$ ($Pr = 0.7$). When W_{om} tends to infinity, β and the heat quantity exchanged tend both to 0: thereby at high frequencies, thermal transfers may vanish. That means the inter-plates distance «*e*» must be reduced to ensure a low value of W_{om} and an adequate thermal exchange (since the thermal boundary layer diminishes with frequency, then radial exchanges become less important than axial diffusivity).

2.3. Case of a linear and time constant wall temperature profile

The wall temperature profile is now given by a linear equation:

$$T_t^*(x^*) = \frac{T_1^* - T_{-1}^*}{2} x^* + \frac{T_1^* + T_{-1}^*}{2} \tag{23}$$

Thermal transfers phenomena are more complicated when a temperature gradient along the plates' walls is imposed: in the case of particles flowing into the exchanger and passing on $-x^* = -1$, the expression of the fluid to wall local temperature difference for x^* and t^* becomes ([17], Eq. (52)):

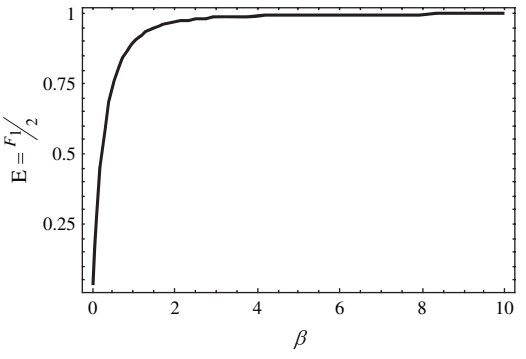

Fig. 4. Exchanger effectiveness representation (corresponding to $F_1/2$) as function of parameter β.

$$\Delta T_{\text{rad}}(t^*, x^*, x_0^*) + \frac{\lambda}{2}\Delta T_{\text{long}} \cos(t^* - \varphi) = \left(\Delta T_{\text{rad}}(t^*, -1) + \frac{\lambda}{2}\Delta T_{\text{long}} \cos(t_{\text{in}}^* - \varphi)\right) e^{-\beta(t^* - t_{\text{in}}^*)} \tag{24}$$

With the phase φ depending on β:

$$\cos\varphi = \frac{\beta}{\sqrt{1+\beta^2}};\ \sin\varphi = \frac{1}{\sqrt{1+\beta^2}} \tag{25}$$

And the time interval when a fluid particle remains in the canal is given by:

$$t_{\text{in}}^* = \arcsin\left[-1 - \frac{(1 + x_0^*)}{\Lambda_L}\right];\ \text{and}\ t_{\text{out}}^* = \pi - t_{\text{in}}^* \tag{26}$$

Let us now express the wall extremities temperature difference (constant) by:

$$\Delta T_{\text{long}} = T_1^* - T_{-1}^* \tag{27}$$

According to the wall temperature profile (Eq. (23)), the fluid to wall temperature difference in Lagragian formulation is:

$$\Delta T_{\text{rad}}(t^*, \xi) = \overline{T}_g^*(t^*, \xi) - \overline{T}_t^*(x^*) \tag{28}$$

It is always depending on the position $\xi = x^* - \lambda \sin t^*$ of the fluid particle at the time t^*, but now local wall temperature varies along x^*.

Eq. (24) is valid only for particles never exiting at $x^* = 1$ and over times $t^* \in [t_{\text{in}}^*, t_{\text{out}}^*]$. So the two temperature differences $\Delta T_{\text{rad}(-1)}$, $\Delta T_{\text{rad}(1)}$ and the wall extremities temperature difference ΔT_{long} both contribute to the variation of the fluid temperature profile; moreover an exponential decrease of parameter β still occurs.

For fluid particles flowing back into the system and passing through the inlet section at $x^* = 1$ ($\Delta T_{\text{rad}}(t^*, 1) = -0.25$ on Fig. 5), the following relation must be applied:

$$\Delta T_{\text{rad}}(t^*, x^*, x_0^*) = -\frac{\lambda}{2}\Delta T_{\text{long}}\left(\cos(t_{\text{in}'}^* - \varphi) e^{-\beta(t^* - t_{\text{in}'}^*)} - \cos(t^* - \varphi)\right) + \Delta T_{\text{rad}}(t^*, 1) e^{-\beta(t^* - t_{\text{in}'}^*)} \tag{29}$$

With the time interval:

$$t_{\text{out}'}^* = \arcsin\left[-1 + \frac{(1 - x_0^*)}{\Lambda_L}\right];\ \text{and}\ t_{\text{in}'}^* = \pi - t_{\text{out}'}^* \tag{30}$$

Fig. 5 shows temperature profiles histories obtained along the plates within the fluid for the same three relative displacements Λ_L and assuming the fluid inlet temperature is the same of Fig. 3 (so $\Delta T_{\text{rad}}(t^*, 1) = -0.25$ and $\Delta T_{\text{rad}}(t^*, -1) = +0.25$ in order to respect this hypothesis). Whatever Λ_L and β values, the existence of a thermal gradient along the walls induces the ''regenerator'' effect for thermal exchanges as explained in the first part of this work. A part of the heat quantity exchanged between gas and wall may be restituted in the second half period; for example, this situation must be avoided in the case of a cooler

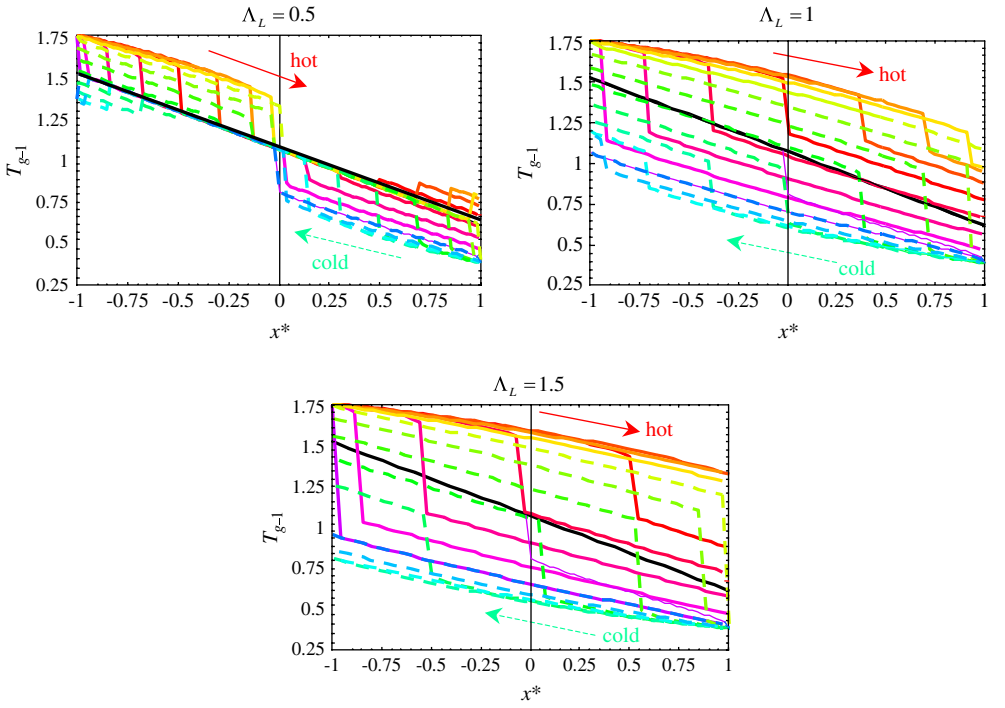

Fig. 5. Histories of the non-dimensional temperature profile along the exchanger $[-1, +1]$ and of the relative fluid displacement, case of a linear profile of the wall temperature $\Delta T_{\text{long}} = 0.5$ (thick line). Hot fluid inlet $\Delta T_{\text{rad}(-1)} = +0.25$ on the left on the first half alternation, and cold fluid inlet on the right $\Delta T_{\text{rad}(1)} = -0.25$ on the reciprocating flow. Full lines represent a flow period from $x^* = -1$ to $x^* = +1$, dotted lines in the other way $-\beta = 0.5$ and $Pr = 0.7$. $\Lambda_{\text{L}} = 1$ stands for heat exchanger where displacement of fluid is equal to exchanger length, $\Lambda_{\text{L}} < 1$ for long exchangers and $\Lambda_{\text{L}} > 1$ for short exchangers.

exchanger. After the flow direction change, the fluid particles that are colder than the wall (located under the thick line of wall temperature in Fig. 5) have a reversed heat exchange because they move along a positive thermal gradient hence the fluid is heated back. That is the reason why this process can be qualified as a wall "regenerator effect". At the same time, particles that are still hotter than the wall cool anymore. When the thermal gradient through the wall is negative, the regenerator effect is added to the exponential decrease of the "entrance" temperature gradient. In the particular case where $\Delta T_{\text{rad}(+1)}$ is strictly symmetric to $\Delta T_{\text{rad}(-1)}$ with respect to wall temperature (case of Fig. 5), the global thermal balance becomes null and the exchanger operates as a regenerator actually; on the contrary if $\Delta T_{\text{rad}(+1)}$ and $\Delta T_{\text{rad}(-1)}$ are of the same sign, thermal exchanges are doubled.

Calculus of the exchanged heat quantities leads to distinguish two cases depending upon the exchanger length: short $(\Lambda_{\text{L}} > 1)$ and adapted or long $(\Lambda_{\text{L}} < 1)$:

- case of adapted or long exchangers $(\Lambda_{\text{L}} < 1)$, with $\Delta T_{\text{rad}(+1)} = 0$

$$Q_{\Lambda_{\text{L}} \le 1} = Q_{\text{rad}} = \rho c_{\text{g}} S_{\text{pass}} \frac{l_0}{2} T_0 \Delta T_{\text{rad}(-1)} \Lambda_{\text{L}} F_1(\beta) \tag{31}$$

- case of short exchangers $(\Lambda_{\text{L}} > 1)$, with $\Delta T_{\text{rad}(+1)} = 0$

$$Q_{\Lambda_{\text{L}} > 1} = \rho c_{\text{g}} S_{\text{pass}} \frac{l_0}{2} T_0 \Delta T_{\text{rad}(-1)} (Q_{11} + Q_{21}) - \rho c_{\text{g}} S_{\text{pass}} \frac{l_0}{2} T_0 \frac{\lambda}{2} \Delta T_{\text{long}} (Q_{12} - Q_{p1}) \tag{32}$$

Note: if $\Delta T_{\text{rad}(+1)} \neq 0$, one must add a supplementary term similarly to $\Delta T_{\text{rad}(-1)}$

Terms Q_{11}, Q_{12}, Q_{21},…,Q_{p1} are demonstrated and calculated in Ref. [17] (Eqs. (62), (63) and (65)). They correspond to integral heat quantities exchanged for particular volume of fluid during each half period (fluid on the left or on the right or inside of the plate system at initial time, Fig. 2).

Once again the evolutions of the right member terms of Eq. (32) still have been represented on Figs. 8 and 9 of Ref. [17]. The term $(Q_{11} + Q_{21})$ represents a degradation factor of the efficiency (with respect to the case of an exchanger of sufficient length) because the ratio $(Q_{11} + Q_{21})/\Lambda_{\text{L}} F_1$ is always inferior to one. Its value is lower especially when Λ_{L} increases and β decreases (large W_{om}): therefore, in the case of a too short exchanger, the thermal exchange is not efficient. Otherwise the last term $(Q_{12} - Q_{p1})$ remains always negative and decreases when Λ_{L} increases. The regenerator effect and the exchanged-restituted energy parts

are characterized by this second term in Eq. (32). The global sign of the second term of Eq. (32) depends on the sign of the temperature difference ΔT_{long}.

2.4. Fluid inlet temperature depending on time

The functioning of machines like Stirling, Vuilleumier, Gifford-Mc Mahon, Pulse Tube Refrigerator or thermo-acoustical systems is often quite different from conditions previously described; it may be characterized by:

- the use of a compressible fluid,
- the flow is usually turbulent,
- fluid and materials physical properties may strongly vary (at cryogenic temperatures for example),
- periodic fluctuations and phase lag fluctuations of thermodynamic quantities: pressure, temperature, displacement, velocity, etc.
- the amplitude of these fluctuations that may not match the linear thermoacoustic theory.

When $\Delta T_{\text{rad}(-1)}$ and $\Delta T_{\text{rad}(+1)}$ vary over time sinusoidally (like in Stirling machines for example), the previous expression of $F_1(\beta)$ appears as a function of the phase lag between the temperature and the inlet velocity. Therefore both its integration and that of initial Eq. (16) become more complicated actually.

Let now pay attention onto the modifications that must be applied to previous results in the specific following case: the fluid inlet temperature at the device extremities varies over time and its phase lag with the fluid velocity variations is φ_{T}. This temperature variation is supposed of the following periodic form:

$$\Delta T_{\text{rad}} = \Delta T \frac{\left(1 - \cos\left(t^*_{\text{in}}\left(x^*_0\right) - \varphi_{\text{T}}\right)\right)}{2} \tag{33}$$

Note: velocity is still $\overline{u}^* = \cos t^*$ and in Lagrangian formulation t^*_{in} and x^* depend both on the initial particle position x^*_0.

Fig. 6 illustrates the thermal front of the fluid, along the canal at different instants over a period and for a particular value of the temperature phase $\varphi_{\text{T}} = (\pi/2)$. For simplicity, the case of a null ΔT_{long} is chosen; otherwise the regenerator effect still exists and is not influenced by the variation of the fluid inlet temperature. One can note the important difference existing in comparison with the previous graphs of Fig. 3. The graphic representation is the same: full lines stand for each instant when fluid flows from $x^* = -1$ to $x^* = +1$, and dotted lines in the other way. Horizontal arrows symbolize the fluid displacement; vertical arrows represent the variation of the fluid inlet temperature amplitude at the same time. One clearly observes the combination at side $x^* = -1$ of the diminution of the inlet temperature during the displacement of the fluid toward the left and the exponential diminution of

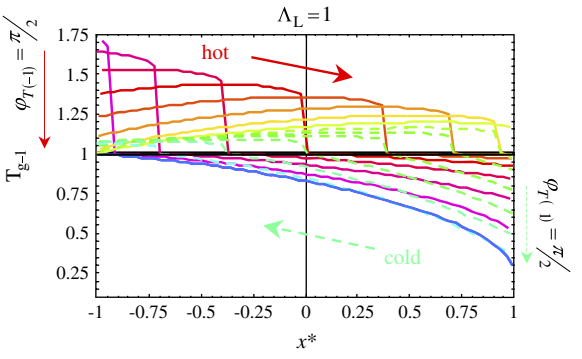

Fig. 6. Temperature profiles histories when the inlet fluid temperature varies over time for a heat exchanger where displacement of fluid is equal to exchanger length $\Lambda_{\text{L}} = 1$. Case of a constant wall temperature $\Delta T_{\text{long}} = 0$ (horizontal thick line). Hot fluid inlet amplitude $\Delta T_{\text{rad}(-1)} = +0.25$ and phase $\varphi_{T-1} = \pi/2$ on the left for the first half alternation, and cold fluid inlet on the right $\Delta T_{\text{rad}(1)} = -0.25$ and phase $\varphi_{T+1} = \pi/2$ for the reciprocating flow. Full lines represent a flow period from $x^* = -1$ to $x^* = +1$, dotted lines in the other way. Vertical arrows indicate the time inlet temperature evolution of the fluid $-\beta = 0.5$ and $Pr = 0.7$.

the hot thermal front due to thermal transfer with the wall. After the alternation of the fluid, the temperature of the cold fluid drops as long as the fluid is entering at $x^* = +1$ while the heat transfer between the wall and the hot fluid is going on. When evaluating the heat quantities, only the terms related to the previously constant temperature difference $\Delta T_{\text{rad}(-1)}$ have to be substituted by Eq. (33), thermal exchange phenomenon due to the gradient ΔT_{long} being not affected.

Fig. 7 shows the new term related to exchanger efficiency that replaces the value $\Lambda_{\text{L}} F_1(\beta)$ in Eq. (31) for long or adapted exchangers; it is reported in a 3D graphic as function of the phase lag φ_{T} and phase thermal transfer parameter β: A section of the graph in the plane

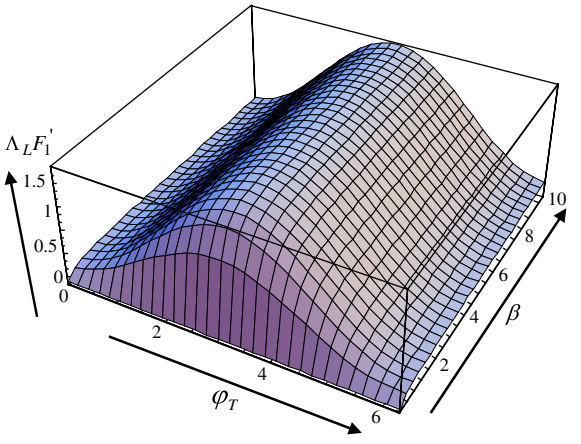

Fig. 7. Efficiency factor $\Lambda_{\text{L}} F'_1$ as a function of β and of the phase lag φ_{T} between the gas temperature and the fluid velocity.

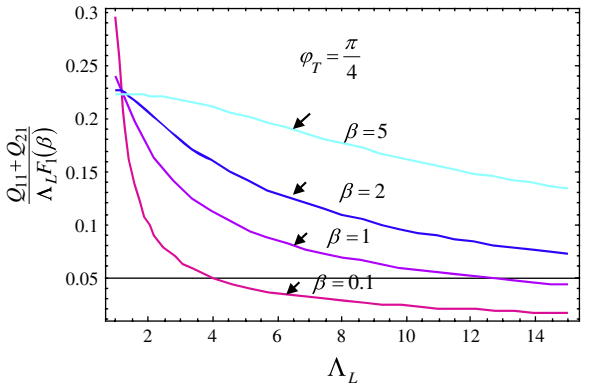

Fig. 8. Corrective term of heat quantities $(Q_{11}+Q_{21})/(\Lambda_L F_1(\beta))$ as a function of Λ_L ($\Lambda_L > 1$ and $\varphi_T = \pi/4$).

$\varphi_T = \text{const}$ shows that the evolution is similar to that of efficiency in Fig. 4, however, according to φ_T the maximal value is very different, and even null if $\varphi_T = 0$. "β" still has to be chosen as high as possible, in order to limit the Womersley number.

$$\Lambda_L F_1' = \Lambda_L \frac{\cos^2\varphi_T e^{-2\beta\pi}[C1 - C2]}{C3} \tag{34}$$

With:

$$C1 = \left(1+4\beta^2\right)\left(1+e^{2\beta\pi}\left(2\beta^3\pi+2\beta\pi-1\right)\right)\cos\varphi_T$$

$$C2 = \beta\left(4\left(1+\beta^2\right)\left(\left(1+8\beta^2\right)e^{2\beta\pi}-1\right) + \left(1+4\beta^2\right)\left(e^{2\beta\pi}-1\right)\sin\varphi_T\right)$$

$$C3 = 8\beta^2\left(1+5\beta^2+4\beta^4\right)\left(\sin^2\varphi_T - 1\right)$$

The correction term $Q_{11}+Q_{21}$ of heat exchange efficiency for short exchangers (Eq. (32)) has also to be modified. Only numerical values can be obtained: an example of the relative value compared to $\Lambda_L F_1(\beta)$ for a temperature phase lag of $\varphi_T = 45°$ is given in Fig. 8. In comparison with Fig. 8 of [17], the values are quite lower in comparison with the case of a long exchanger of constant parietal temperature.

3. Average density of enthalpy flux

A good criterion for evaluating thermal exchanges between fluid and wall in an exchanger operating in a periodic flow regime consists in observing the variations of the local and time averaged enthalpy flux $\dot{h} = \rho_g c_g u T$ and $\dot{H} = (\omega/2\pi)\int_0^{2\pi/\omega}\dot{h}(t)\mathrm{d}t$. In dimensionless form and for the first order, i.e. with a constant density, $\dot{h}^*$ and its average value $\dot{H}^*$ can be expressed as following:

$$\dot{h}^* = \rho^* u^* T_g^* = \frac{2\dot{h}}{\omega D \rho_0 T_0 c_g} \text{ and } \dot{H}^* = \rho^*\left\langle u^* T_g^*\right\rangle = \frac{2\dot{H}}{\omega D \rho_0 T_0 c_g} \tag{35}$$

The goal with a heat exchanger is to maximize the variations of the average enthalpy flux between the two device extremities (an increase in a heater, a decrease in a cooler). The 1D averaged model developed here makes easy the study of heat exchangers in oscillating flow mode, but conditions of real functioning being complicated, the understanding of phenomena remains sometimes fragmentary: boundary conditions, phase lags, temperature profiles, etc.

Fig. 9 shows axial variations of the average enthalpy $\dot{H}^*$ for different kinds of exchangers operating with or without a thermal gradient at the wall (same values to those of Fig. 5). Variations of $\dot{H}^*$ are more significant if there is an increase of β, taken to 0.5 for example. For an exchanger in which length represents twice the displacement value, half the device does not contribute to heat exchanges: indeed, in such a case, the global thermal behavior is similar to that found for $\Lambda_L = 1$. With a too short exchanger, global

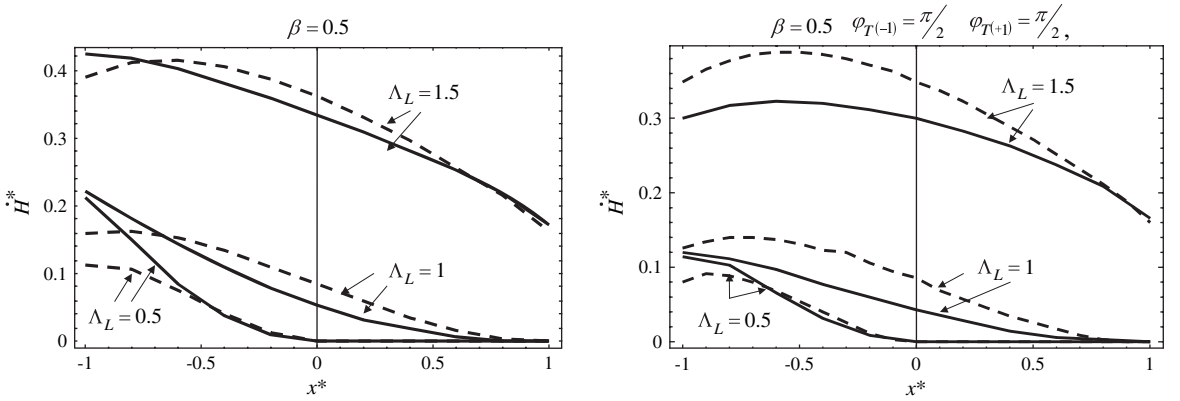

Fig. 9. Axial variation of the average enthalpy $\dot{H}^* = \rho^*\langle u^* T_g^*\rangle$ for different kind Λ_L of exchangers of uniform wall temperature ($\beta = 0.5$), full lines $\Delta T_{long} = 0$, dotted lines $\Delta T_{long} = 0.5$ left: constant inlet temperatures, right: variable over time inlet temperatures with phase lag 90° on both sides.

variations of $\dot{H}^*$ are not very different, however, temperature levels need to be higher and the axial profile form is very different. Eventually, the thermal gradient in the wall (negative in the above example) induces a decrease of $\dot{H}^*$ in all cases. Influence of phases of inlet temperatures is more difficult to explain: in the chosen example, it is clear that enthalpy level diminishes because average inlet temperatures also diminish.

4. Conclusions

It has been demonstrated for oscillating fluid flows that classical formulations of thermal heat transfer evaluations, and especially those corresponding to steady fluid flows regime, cannot be employed. This is a consequence of the phase lag existing between all the physical variables (pressures, displacements, velocities, temperatures, etc.) and the energy transfers. This is also a consequence of the particular interaction between the wall profile temperature and the oscillation of the fluid.

Two important parameters (in addition to Prandtl number) characterize oscillating flow thermal transfers: Λ_L, the ratio between fluid displacement and heat exchanger length, and the Womersley number W_{om} depending on the oscillating frequency and the hydraulic radius. The model studied in this paper allows the calculation of the thermal effectiveness ($F_{1/2}$) of heat exchanger with incompressible oscillating flows; this is a first step because compressible flows are too complicated for our current knowledge. Corrections functions are given for the case of short heat exchangers $\Lambda_L > 1$, when a longitudinal gradient exists $\Delta T_{long} \neq 0$, or when fluid inlet temperatures are time dependent.

Meanwhile, conclusions are still interesting:

- it is unprofitable to use too large or too short heat exchangers, better performances are obtained when there is adaptation between length and fluid displacement;
- when a temperature gradient is present along the wall of the exchanger, the efficiency can be dramatically diminished by a ''regenerator effect''.

The last remark is particularly important for designers of heat exchangers, Womersley numbers superior to 1.3, corresponding to $\beta < 2$ (case $Pr = 0.7$), are prohibited because the thermal efficiency dramatically vanishes, so hydraulic radius have to be adjusted according to the operating frequency.

Appendix 1. Complete expressions of exchange and friction coefficient

Plates:

$$Nu = \frac{4jPrW_{om}^2 \tanh(W_{om}\sqrt{jPr})}{W_{om}\sqrt{jPr} - \tanh(W_{om}\sqrt{jPr})},\quad C_f Re = \frac{8jW_{om}^2 \tanh(W_{om}\sqrt{j})}{W_{om}\sqrt{j} - \tanh(W_{om}\sqrt{j})}$$

Tubes:

$$Nu = -2W_{om} j^{3/2}\sqrt{Pr}\frac{J_1\left(W_{om}\sqrt{Pr}j^{3/2}\right)}{J_0\left(W_{om}\sqrt{Pr}j^{3/2}\right) - 1},\quad C_f Re = 4W_{om} j^{3/2}\left(\frac{2}{W_{om}j^{3/2}} - \frac{J_0(W_{om}j^{3/2})}{J_1(W_{om}j^{3/2})}\right)^{-1}$$

Table 1
Main dimensionless numbers characterizing oscillating fluid flows (from 1D model)

Numbers definitions	Name	Signification
$\Lambda_L = \frac{D}{l_0}$	Non-dimensional ratio	Ratio of total acoustical displacement to axial length Important for extremities effects if D is large in front of l_0
$W_{om} = \sqrt{\frac{\rho_0 \omega r_h^2}{\mu}}$	Womersley/Stokes	Ratio of hydraulic radius to viscous diffusion thickness
$M_\omega = \frac{\omega D}{\sqrt{p_0/\rho_0}}$	Mach	Ratio of acoustical velocity to sound velocity Acoustic effects, variable compressibility effects to be considered If $M_\omega > 0.1$ non-linearity of the phenomenon
$Pr = \frac{c_g \mu}{\lambda_g}$	Prandtl	Ratio of viscous and thermal diffusion length
$C_f R_e$	Darcy Product	Characterizes local frictions on walls
$Nu_{R1} = \frac{2e\Re[h]}{\lambda_g}$	Real Nusselt	Characterizes the external thermal transfer
$Nu_{I1} = \frac{2e\Im[h]}{\lambda_g}$	Imaginary Nusselt	Characterizes the internal thermal transfer into walls

References

[1] G.Y. Reader, C. Hooper, Stirling Engines, E. & F.N. Spon, London, New York, 1983.

[2] W.T. Beale, Free piston engines, some model tests and simulations, in: Int. Automotive Engineering Congress, Detroit Mich., January 13–17, n° 690230, 1969.

[3] J.R. Senft, Ringbom Stirling engines, Oxford University Press, New York, 1993.

[4] R. Radebaugh, Pulse tube refrigeration, a new type of cryocooler Proceedings of the 18th International Conference on Low Temperature Physics, Kyoto, 1987, Japan, J. of Appl. Phys. 26 (Suppl. 26-3) (1987) 2076–2081.

[5] R. Radebaugh, A review of pulse tube refrigerator, Adv. Cryogenics Eng. 35 (1990) 1191–1205.

[6] P.H. Ceperley, A pistonless Stirling engine, the traveling wave heat engine, J. Acoust. Soc. Am. 66 (1979) 1513.

[7] S. Schulz, B. Thomas, Experimental investigation of a free-piston Vuilleumier refrigerator, ReV. Int. Froid 18 (1) (1995) 51–57.

[8] C.D. West, Liquid Piston Striling Engines, Van Nostrand Reinhold, New York, (1983) 7–27.

[9] C.W. Stammers, The operation of the fluidyne heat engine at low differential temperatures, J. Sound Vib. 63 (54) (1979) 507–516.

[10] G. Walker, Cryocoolers. Part 1 and 2, Pleonum Press, New York, London, 1983.

[11] G. Walker, Miniature Stirling cryocoolers: trends in development, Cryogenics 26 (July, 1986) 387–391.

[12] D. Gedeon, Mean-parameter modeling of oscillating flow, J. Heat Transfer 108 (1986) 513–518.

[13] G.W.Swift, Thermoacoustics: a unifying perspective for some engines and refrigerators, Fifth draft LA UR 99 895 29, May 2001.

[14] R.S. Wakeland, R.M. Keolian, Thermoacoustics with idealized heat exchangers and no stack, J. Acoust. Soc. Am. 111 (6) (2002) 2654–2664.

[15] R.S. Wakeland, R.M. Keolian, Effectiveness of parallel-plate heat exchangers in thermoacoustic devices, J. Acoust. Soc. Am. 115 (6) (2004) 2873–2886.

[16] R.S. Wakeland, R.M. Keolian, Calculated effects of pressure driven temperature oscillations on heat exchangers in thermoacoustic devices with and without stack, J. Acoust. Soc. Am. 116 (1) (2004) 294–302.

[17] P. Nika, Y. Bailly, F. Lanzetta, Transferts thermiques en écoulements oscillants laminaires imcompressibles, Int. J. Refrigeration 28 (2005) 353–367.

[18] P. Nika, Y. Bailly, F. Guermeur, Thermoacoustics and related oscillatory heat and fluid flows in micro heat exchangers, Int. J. Heat Mass Transfer 48 (2005) 3773–3792.

[19] A.A. Khornauser, J.L. Smith, Application of a complex Nusselt Number to heat transfer during compression and expansion, Trans. ASME 116 (August 1994) 536–542.